Carbohydrate Polymers 90 (2012) 1494–1500

Contents lists available at SciVerse ScienceDirect

Carbohydrate Polymers

journal homepage: www.elsevier.com/locate/carbpol

In vitro evaluation of an RGD-functionalized chitosan derivative for enhanced cell adhesion

Annasara Hansson[a,b,c], Nour Hashom[a], Françoise Falson[c], Patricia Rousselle[b], Olivier Jordan[a], Gerrit Borchard[a,*]

[a] School of Pharmaceutical Sciences, University of Geneva, University of Lausanne, Quai Ernest Ansermet 30, 1211 Geneva, Switzerland
[b] SFR BioSciences Gerland-Lyon Sud, Institut de Biologie et Chimie des Protéines, FRE 3310, CNRS; Université Lyon 1, 7 passage du Vercors, 69367 Lyon, France
[c] Faculty of Pharmacy, University Claude Bernard Lyon 1, 8 Ave Rockefeller, 69373 Lyon, France

ARTICLE INFO

Article history:
Received 21 April 2012
Received in revised form 30 June 2012
Accepted 7 July 2012
Available online 14 July 2012

Keywords:
Wound healing
Human dermal fibroblast
Chitosan
RGD peptide
Cell adhesion

ABSTRACT

Tissue repair is a spontaneous process that is initiated on wounding. However, if this complex mechanism is impaired or not sufficient the use of biomaterials might increase the chance of successful healing. In this view, an RGD-functionalized polymer was developed to promote dermal healing. A water-soluble chitosan derivative, carboxymethyl-trimethylchitosan (CM-TM-chitosan) was synthesized and GRGDS-moieties were grafted to the backbone at a concentration of 59 nmol/mg polymer to increase cell–biomaterial interaction. Tested *in vitro* with cultured human dermal fibroblasts, the developed polymer showed good biocompatibility and the initial adhesion was increased by 3–5 times due to the GRGDS-moieties. Moreover, cell spreading was specific to the interaction with GRGDS, giving a 12-fold increase of cells showing a fully spread morphology within 30 min. Overall, CM-TM-chitosan conjugated with GRGDS-peptides may prove useful as a biomaterial in wound healing.

1. Introduction

In wound healing and tissue engineering, infiltration of cells into and over the wound site is critical. Therefore cell adhesion- and migration-promoting properties of biomaterials are decisive. *In vivo*, cells are surrounded by the extracellular matrix (ECM), a hydrated network of proteins and proteoglycans that provide structure and guidance for the cells in most vital processes (Hynes, 2009). Collagens, and glycoproteins such as laminins and fibronectins are biologically active proteins present in the ECM with important roles in the regulation of cell adhesion and migration. It has been shown that short amino acid sequences in these proteins, interacting with specific cell receptors, are responsible for the induction of cell responses. Examples of peptide sequences shown to be able to induce adhesion in various cell types are YIGSR from laminin (Graf et al., 1987), GFOGER from collagen (Knight, Morton, Peachey, Tuckwell, Farndale & Barnes, 2000) and RGD, first identified in fibronectin (Pierschbacher & Ruoslahti, 1984). Developing hybrid biomaterials equipped with such peptide sequences represents an attractive alternative to confer functionality improving cell–biomaterial interaction.

The amino acid sequence RGD (arginine-glycin-aspartic acid), is a tripeptide found in ECM proteins such as fibronectin, vitronectin and laminin (Hersel, Dahmen & Kessler, 2003). RGD is known to induce adhesion and migration through interaction with several members of the integrin family, *e.g.*, αV-integrins, αIIbβ3, α5β1 and α8β1 (Danen & Sonnenberg, 2003). The binding between RGD and the integrin triggers the Rho GTPase pathway, regulating the rearrangement of the cytoskeleton (Huveneers & Danen, 2009), resulting in the initiation of cell spreading, adhesion and migration.

Due to its reported biocompatibility, biodegradability and its ease of modification, chitosan has been widely investigated for its biomedical and pharmaceutical application (Alves & Mano, 2008; Amidi, Mastrobattista, Jiskoot & Hennink, 2010; Baldrick, 2010; Muzzarelli, Greco, Busilacchi, Sollazzo & Gigante, 2012; Muzzarelli, 2009, 2011). Chitosan is a co-polymer composed of randomly distributed D-glucosamine and N-acetyl-D-glucosamine monomers (Jollès & Muzzarelli, 1999; Muzzarelli & Muzzarelli, 2005). Derivatives of chitosan been synthesized with success, tailoring its properties such as increased water solubility or adding a permanent positive or negative charge, for various applications (Muzzarelli, 1988). Moreover, chitosan has been shown to favor wound healing at several different stages. It was reported to have hemostatic activities through activation of platelets (Lord, Cheng, McCarthy, Jung & Whitelock, 2011) and moreover, an increased

Abbreviations: TM-chitosan, trimethyl chitosan; CM-TM-chitosan, carboxymethyl-trimethyl chitosan; RGD, Arg-Gly-Asp; GRGDS, Gly-Arg-Gly-Asp-Ser; SDGRG, Ser-Asp-Gly-Arg-Gly.

* Corresponding author. Tel.: +41 22 379 3802; fax: +41 22 379 6567.
E-mail address: gerrit.borchard@unige.ch (G. Borchard).

0144-8617/$ – see front matter © 2012 Elsevier Ltd. All rights reserved.
http://dx.doi.org/10.1016/j.carbpol.2012.07.020

infiltration of inflammatory cells and a higher angiogenic activity promoting wound healing, has been observed in wounds treated with chitosan (Boucard et al., 2007; Scherer et al., 2009).

Due to its intrinsic wound healing promoting properties, chitosan and its derivatives have been extensively investigated as a biomaterial for soft tissue repair, alone and in combination with other polysaccharides and glycosaminoglycans (Boucard et al., 2007; Denuziere, Ferrier, Damour & Domard, 1998; Murakami et al., 2010; Takei, Nakahara, Ijima & Kawakami, 2012). During wound healing, the two major cell types, keratinocytes and fibroblasts, proliferate and change their phenotype to the migratory state (Li, Fan, Chen & Woodley, 2004). They enter the wound site to reconstruct the new tissue. Fibroblasts interact with RGD-sequences, mainly through αVβ3 integrins (Massia & Hubbell, 1991). Scaffolds and polymeric gels functionalized with RGD-sequences are therefore attractive alternative adhesion/migration-promoting substrates to enhance dermal repair. In this view, we have developed a chitosan derivative functionalized with GRGDS-moieties for use in formulations such as polyelectrolytic complexes, gels and layer-by-layer coatings with the aim to promote wound healing.

2. Materials and methods

2.1. Materials

For synthesis, chitosan (ChitoClear Cg10, 7 and 15 mPa s) was bought from Primex, (Siglufjordur, Iceland), GRGDS- and SDGRG-peptides from Bachem (Bubendorf, Switzerland), dialysis membranes from Spectra (Breda, The Netherlands) and syringe filters from Millipore AG (Zug, Switzerland). For *in vitro* bioactivity assays, cell culture media and additives were obtained from PAN Biotech GmbH (Aidenbach, Germany) and plastics from Corning (Amsterdam, The Netherlands). The XTT cell proliferation kit 2 was bought from Roche (Basel, Switzerand). For immunofluorescence staining, phalloidin conjugated Alexa 488 was bought from Lonza (Basel, Switzerland), Vectashield mounting medium from Vector Laboratories (Peterborough, UK) and paraformaldehyde from Alfa Aesar (Ward Hill, MA, USA). All other chemicals and reagents were bought from Sigma–Aldrich (Buchs, Switzerland).

2.2. Synthesis of GRGDS-CM-TM-chitosan

2.2.1. Trimethylation of chitosan

Trimethylation of chitosan was achieved through nucleophilic substitution by methyl iodide (MeI) using a modified protocol by Heuking, Iannitelli, Di Stefano, and Borchard (2009), shown in Fig. 1. Briefly, chitosan was suspended in 1-methyl-2-pyrrolidinone (NMP; 40 ml NMP/g chitosan) and the suspension was kept at pH 10 by addition of NaOH 15%. MeI (6 ml MeI/g chitosan) was added and the mixture let react under a reflux condenser at 60 °C for 100 min. After filtration on a P3 glass filter, the resulting trimethyl-chitosan (TM-chitosan) was precipitated and washed twice with 5 volumes of a mixture of diethyl ether and ethanol (1:1, v/v). The final product was solubilised in 10% NaCl and purified by dialysis using a Spectra/Por 4 dialysis membrane with a molecular weight cut-off of 12–14 kDa over three days before lyophilization.

2.2.2. Carboxymethylation of trimethylchitosan

To obtain CM-TM-chitosan, the freeze-dried TM-chitosan was suspended in NMP (10 ml NMP/100 mg TM-chitosan) at room temperature overnight. The pH was readjusted to a value of 10 with NaOH 15% before adding chloroacetic acid (20 mol equivalents/TM-chitosan sugar unit). The pH was kept constant at a value of 10 during the whole reaction. After 3 h the resulting carboxymethyl-trimethyl-chitosan (CM-TM-chitosan) was precipitated in 5 volumes of a mixture of diethyl ether and ethanol (1:1, v/v) and washed twice. The CM-TM-chitosan was solubilized in Milli-Q water and the pH was adjusted to a value of 5 by the addition of 5 N HCl, before being filtered through a 0.45 μm syringe filter. Dialysis was performed as described for TM-chitosan, over three days while changing the water three times per day. The purified product was lyophilised for storage.

2.2.3. Conjugation of GRGDS to carboxymethyl-trimethyl chitosan

In the last step, the GRGDS peptide was grafted to a CM-TM-chitosan backbone *via* the carboxyl group by a carbodiimide reaction. First, CM-TM-chitosan was dissolved in MilliQ water and the pH was adjusted to neutral. Thereafter, 5 mol equivalents to the carboxyl groups of CM-TM-chitosan of N-(3-dimethylaminopropyl)-N′-ethylcarbodiimide hydrochloride (EDC) and N-hydroxysuccinimide (NHS) each, were added to activate the carboxyl groups of CM-TM-chitosan. The pH was readjusted to a value of 7 and the mixture was left for 1 h. The GRGDS- and SDGRG-peptide respectively, dissolved in MilliQ-water were added and the reaction was performed over a time period of 96 h with the pH being maintained at a value of 7. The finalized product was adjusted to pH 3 by adding HCl 1 N and filtered through a 0.45 μm syringe filter. Before being lyophilized for storage, the polymer was purified by dialysis for 3 days. The water was changed three times per day. The total yield of the reaction was 0.67 ± 0.06 ($n = 3$ batches), and the yields of peptide grafting were 0.12 for GRGDS-CM-TM-chitosan and 0.10 for SDGRG-CM-TM-chitosan, as characterized by amino acid analysis (AAA).

2.3. Characterization of polymer

2.3.1. ^{1}H nuclear magnetic resonance

^{1}H nuclear magnetic resonance (NMR) spectra were obtained with a Varian Gemini 300 MHz spectrometer (Agilent Technologies, Santa Clara, CA, USA). All compounds were dissolved in D_2O or in 0.1% DCl in D_2O. The samples were analyzed at 25 °C. Chemical shifts (δ) are relative to the internal standard 3-trimethylsilyl propionic acid-d_4 sodium salt (TSP; $\delta = 0.0$ ppm for ^{1}H). The shifts were assigned as follows (An, Thien, Dong, & Dung, 2009; Hjerde, Vårum, Grasdalen, Tokura, & Smidsrod, 1997): $NCOCH_3$ (δ 2.1), $N(CH_3)_3$ (δ 3.3), NCH_2COOH (δ 3.95), OCH_2COOH (δ 4.35) in position 6 and OCH_2COOH (δ 4.5) in position 3.

The degrees of substitution (DS) for N-acetylation, N-trimethylation and N-and O-carboxymethylation were determined. To estimate the fraction of monomers substituted with N-acetyl groups, trimethyl- and carboxymethyl groups the following equation was used:

$$\mathrm{DS} = \frac{[\text{substituent}]}{[\mathrm{H}]} \times \frac{1}{n}$$

where [H] is the integral value of the H-1 peaks between 5 and 5.6 ppm, [substituent] the integral value of the group and n the number of equivalent protons present in the substituted group.

2.3.2. Fourier transform infrared spectroscopy

Fourier transform infrared (FTIR) analysis was performed using a PerkinElmer Spectrum 100 FTIR spectrometer (PerkinElmer, Schwerzenbach, Switzerland). All transmission spectra were recorded in the region of 650–4000 cm^{-1}.

2.3.3. Amino acid analysis

The concentrations of peptides in the samples were determined by quantitative amino acid analysis (AAA) using a Biochrom 30 (Biochrom Ltd., Cambridge, UK). Briefly, the samples were hydrolyzed and separated by an ion exchange column. After post-column derivatization by ninhydrin, the samples were analysed at

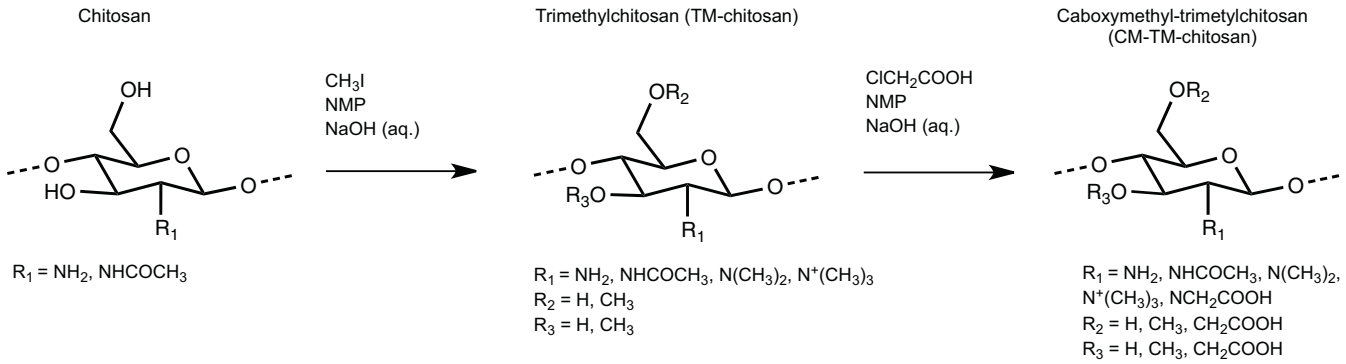

Fig. 1. Synthesis of trimethylchitosan (TM-chitosan), and subsequently carboxymethyl-trimethylchitosan (CM-TM-chitosan), from chitosan in a two-step chemical reaction. Chitosan was trimethylated by a reaction with iodomethyl to form TM-chitosan. TM-chitosan is thereafter carboxymethylated with chloroacetic acid to form CM-TM-chitosan.

wavelengths of 440 and 570 nm. An internal standard of norleucine was used to determine the concentrations of amino acids in the sample.

2.4. Cell culture

Human dermal fibroblasts (HDF) were a kind donation by Dr. Lee Ann Laurent-Applegate (CHUV, Lausanne, Switzerland). The HDF were cultured in Dulbecco's Modified Eagle Medium (DMEM) containing 2 mM glutamine, 10% fetal calf serum and 1% penicillin/streptomycin. The cells were split at sub-confluency with trypsin/EDTA diluted in phosphate buffered saline (PBS). The HDF were used between passages 6 and 10.

2.5. Cytotoxicity

The cytotoxicity of the polymers on HDF was assessed using an XTT-cell proliferation kit 2. Cells were seeded in a 96-well plate at an initial concentration of 10–15 $\times$ 10^3 cells/well. After 24 h the medium was changed to fresh medium containing indicated concentrations of GRGDS- or SDGRG-CM-TM-chitosan. The cells were cultured in the presence of the polymers for 24 h before removing the medium and adding XTT-reagent. The absorbance was measured at a wavelength of 490 nm after 6 h with a Tecan plate reader (Tecan group Ltd., Männedorf, Switzerland) and the cell viability (%) was expressed in percentage relative to a control group of HDF cultured in the absence of either polymer.

2.6. Bioactivity

2.6.1. Adhesion assay

96-well plates (Costar) were coated with GRGDS- or SDGRG-CM-TM-chitosan at indicated concentrations by overnight adsorption at 4 °C. The wells were subsequently saturated with 1% bovine serum albumin (BSA) for 1 h at ambient temperature. The HDF were detached and rinsed in serum-free DMEM before being seeded at a density of 5 $\times$ 10^4 cells/well. After 30 min of incubation (37 °C, 5% CO_2), the non-adhered cells were removed by washing with PBS and the attached cells were fixed for 1 h with a solution of 1% glutaraldehyde in PBS. To evaluate the level of adhesion, the cells were stained for 1 h with a solution of 0.1% crystal violet. After drying, the level of adhesion was determined by solubilizing the dye in 1% acetic acid containing 0.1% Triton-X 100 and measuring the optical density at a wavelength of 570 nm with a Tecan plate reader. For competitive inhibition assays, soluble GRGDS- or SDGRG-peptide (1 mM), were added to the cell suspension 15 min prior to seeding. Cell adhesion assays were then performed as described above.

2.6.2. Immunofluorescence staining

Drops of GRGDS- and SDGRG-CM-TM-chitosan solutions (0.1 mg/ml) were placed on cover glasses and let dry. Once dry, they were placed in Costar 24-well plates and blocked by addition of 1% BSA in PBS for 1 h. Adhesion assays were performed as mentioned in Section 2.6.1. The cells were fixed in pre-warmed PBS containing 4% paraformaldehyde, for 10 min and permeabilized with 0.1% Triton X-100 in PBS for 3 min. Samples were then pre-incubated with 1% BSA in PBS for 20 min to prevent non-specific attachment, before being incubated with 6.6 μM phalloidin conjugated to Alexa 488 in 1% BSA in PBS for 20 min. After being washed in an excess of PBS, the fixed and stained cells were mounted with Vectashield Mounting Medium with 4′,6-diamidino-2-phenylindole (DAPI) before being attached to a microscopic slide. The cell morphology was analyzed with a Zeiss LSM 700 confocal microscope (Carl Zeiss AG, Feldbach, Switzerland) using $\times$10 and $\times$20 objectives.

2.6.3. Spreading analysis

The areas of the spread cells were determined using ImageJ software (available from National Institutes of Health, Bethesda, MD, USA). The surface area of 200–300 cells for each condition and assay were measured. For each condition tested, the mean cell surface was calculated. To analyze the cell morphology, the cells were divided into groups based on their surface. The following size criteria were used; round cells (not spread) <500 μm^2, semi-spread cells 500–1000 μm^2 and spread cells >1000 μm^2. The values were averaged over 5 assays.

2.6.4. Statistical significance

Student's *t* test (for two samples, assuming equal variance) was used to compare data at a significance level of $p < 0.05$. The results were expressed as mean ± standard deviation.

3. Results and discussion

3.1. Characterization of GRGDS-CM-TM-chitosan

The functionalized chitosan derivative was synthesized by three successive steps: trimethylation of the amine groups, an O- and N-carboxymethylation and in a final step the polymer was functionalized with GRGDS-peptide (Fig. 1). The synthesized polymers, TM-chitosan and CM-TM-chitosan, were characterized with respect to the degree of substitution (DS) and the introduction of the new functional groups by ^{1}H NMR.

In Fig. 2, the ^{1}H NMR spectra of TM-chitosan and CM-TM-chitosan are shown. The DS of N-acetylation was determined by the peak at 2.1 ppm in the proton spectra. The degree of acetylation was calculated to be between 0.2 and 0.3, depending on the batch

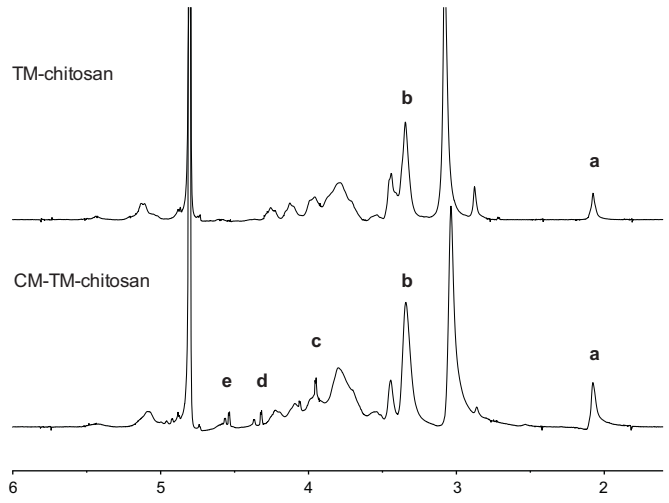

Fig. 2. ^{1}H NMR spectra of TM-chitosan and CM-TM-chitosan. Common for the two spectra are the acetyl- and trimethyl-groups represented by peaks at 2.1 (a) and 3.3 ppm (b), respectively. In the CM-TM-chitosan-spectrum, the peaks at 3.95 (c), 4.35 (d) and 4.55 ppm (e) are corresponding to carboxymethyl-groups in position, 2, 6 and 3, respectively, on the chitosan backbone.

used, values close to those claimed by the provider. The peak at 3.3 ppm (Heuking, Iannitelli, Di Stefano, & Borchard, 2009), present in both spectra, confirmed the N-trimethylation of the chitosan backbone at a DS of 0.4 ± 0.08 ($n = 3$ batches). Similar values were found in the analyses of CM-TM-chitosan. Furthermore, four new peaks appeared in the spectra of CM-TM-chitosan in addition to the functional groups already described for TM-chitosan. Hjerde et al. (1997) reported that the peaks by 3-O- and 6-O-carboxymethyl groups occurred in the range of 4.1–4.6 ppm, and the two peaks at 4.55 and 4.35 were therefore assigned to the carboxymethyl groups in positions 3 and 6, respectively. The peak at 3.95 in the CM-TM-chitosan spectra might be assigned to NCH_2COOH (An, Thien, Dong, & Dung, 2009) and indicated carboxymethylation of the amine in position 2, despite the acetylation and methylation at this position. However, DS in this position is difficult to estimate, since the peak is overlapping with the protons from the carbon ring. Traces of carboxymethyl groups at 4.2 ppm with a carbon resonance at 44.5 ppm (data not shown) were confirmed to be free chloroacetic acid ($ClCH_2COOH$). The total degree of substitution for the carboxymethyl-groups was determined to be 0.15 ± 0.05 in O-6 position and 0.12 ± 0.05 in O-3 position ($n = 3$ batches). Although a higher substitution degree in position O-6 could be expected due to its nature of a secondary alcohol, no significant difference of substitution between the two positions was shown. However, the ratio of substitution in position O-3 and O-6 has shown to change with the water content during the reaction, showing very little or no difference between the positions at certain water/solvent ratio (Chen & Park, 2003), explaining the lack of specificity between the positions.

The results from the NMR-analysis were confirmed by FTIR. Spectra of TM-chitosan, CM-TM-chitosan and GRGDS-CM-TM-chitosan are shown in Fig. 3. The absorption band at 1474 cm^{-1} (CH_3 umbrella) confirmed the introduction of methyl groups on the chitosan backbone for TM-chitosan and its derivatives. Furthermore, the insertion of a carboxyl group in CM-TM-chitosan is confirmed by the new peak at 1750 cm^{-1} (C=O stretch, pH of samples 5–6 when solubilized in water) (Chen & Park, 2003; Pretsch, Bühlmann, & Affolter, 2000). Moreover, the peaks at 1607 cm^{-1} and 1474 cm^{-1} were attributed to asymmetric and symmetric stretch of COO^{-}, respectively, for the moieties in its carboxylate anionic form bound to Na^{+}. Finally, in the spectra of GRGDS-CM-TM-chitosan, the introduction of the amide-bond, formed when grafting the peptide to the backbone, is visible as absorption bands at 1641 (C=O stretch) and 1551 cm^{-1} (N–H bend), both typical for an amide bond. In combination with the NMR-analysis, these

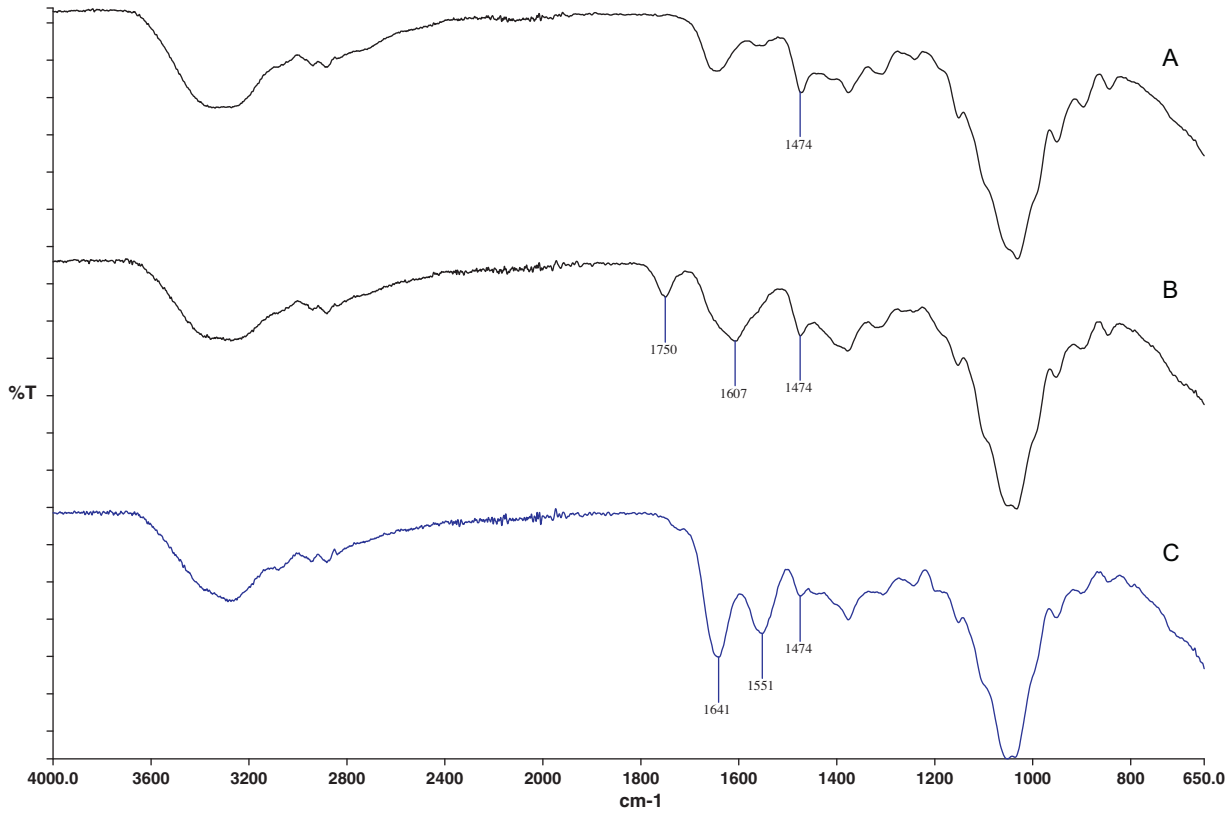

Fig. 3. FTIR-spectra of (A) TM-chitosan; (B) CM-TM-chitosan and (C) GRGDS-CM-TM-chitosan.

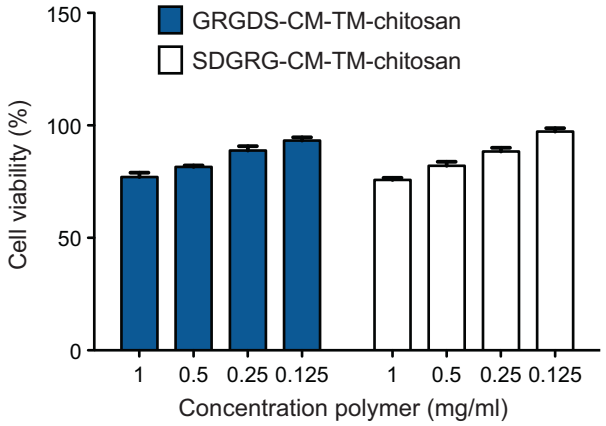

Fig. 4. The cell viability of cultured HDF was assessed by XTT-cell proliferation assays after 24 h in the presence of GRGDS-CM-TM-chitosan and SDGRG-CM-TM-chitosan at indicated concentrations.

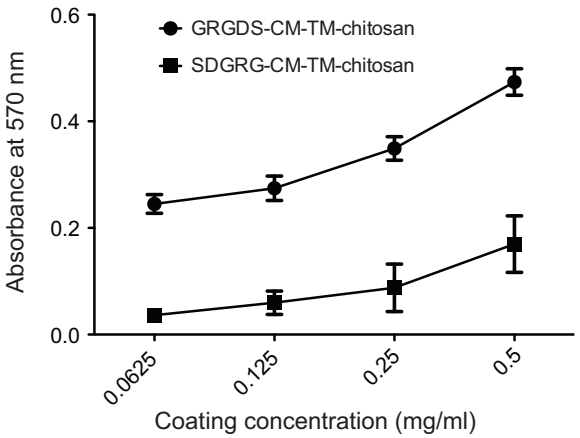

Fig. 5. The level of adhesion after adhesion assays onto coatings of a GRGDS- and SDGRG-CM-TM-chitosan of different concentrations assessed by coloration of the cells and measurements of the absorbance. A 3–5-fold increase of the adhesion onto the polymer containing GRGDS-peptides compared the polymer grafted with SDGRG was observed.

results showed that we successfully synthesized a new polymer, GRGDS-CM-TM-chitosan.

As a final step of the characterization, the level of substitution of peptide to the chitosan backbone was assessed through amino acid analysis (AAA). Two peptides were used, GRGDS and SDGRG. The latter is an inversed RGD-sequence without any biological activity and hence used as a control group to GRGDS. The batches were functionalized with 69 nmol/mg and 59 nmol/mg for GRGDS- and SDGRG-CM-TM-chitosan, respectively. Massia and Hubbell (1991) determined the surface RGD-density needed to induce fibroblast spreading to be 10–10^4 pmol/cm^2. Provided that all GRGDS-moieties are exposed and active in GRGDS-CM-TM-chitosan in a typical adhesion assay, the peptide concentration corresponds to the given range.

3.2. Biocompatibility

The biocompatibility of GRGDS-CM-TM-chitosan and SDGRG-CM-TM-chitosan was tested by initial *in vitro* cytotoxicity tests. Human dermal fibroblasts (HDF) were chosen as a suitable cell model for dermal application. As shown in Fig. 4, a slight decrease of the cell viability was observed at increasing concentrations of the polymers. At the maximal tested concentration of 1 mg/ml, the cell viability was reduced to 75%. However, for the concentrations used in this work no cell viability loss was observed either by GRGDS-CM-TM-chitosan or the control polymer SDGRG-CM-TM-chitosan. Mimicking the conditions used in adhesion assays, toxicity assays were performed on cells seeded onto coatings at different concentrations of GRGDS-CM-TM-chitosan. After 24 h of culture, the cell viability was determined at 98 ± 5% and 95 ± 4% (n = 3 assays) for coatings formed with GRGDS-CM-TM-chitosan of 0.1 and 0.5 mg/ml, respectively. With these results, it was concluded that no adverse effects were shown even after culture on thicker layers of GRGDS-CM-TM-chitosan.

3.3. Bioactivity

To assess the functionality of the GRGDS-peptide after grafting, a series of adhesion assays was performed. In a first step, the adhesion of HDF was tested on increasing coatings of GRGDS grafted polymers. HDF attached in a dose-dependent manner to the coatings (data not shown). In a second step, the scrambled sequence of GRGDS was grafted to CM-TM-chitosan. As shown in Fig. 5, the inactive polymer, SDGRG-CM-TM-chitosan, was used as a negative control in the adhesion assays. An increase in adhesion ranging from threefold for the coating of 0.5 mg/ml, to fivefold for 0.0625 mg/ml was observed in the wells coated with GRGDS-CM-TM-chitosan compared to the SDGRG-CM-TM-chitosan. This demonstrates that the major part of the adhesion is likely to be due to the interaction between integrin receptors and the GRGDS moieties. However, the non-specific adhesion to SDGRG-CM-TM-chitosan is increasing with increasing concentrations of polymer deposited, indicating a second mechanism of interaction between the polymer and cells. Surface properties, such as, polarity, surface charge and surface roughness have been reported to play a role in the attachment of cells to surfaces (Bacakova, Filova, Parizek, Ruml, & Svorcik, 2011). Seen the slightly cationic properties of the derivative, and the negative surface charge of the cells, the cell-coating interaction is attributed to be of electrostatic character. This theory is supported by the well-documented mucoadhesive properties of chitosan, and its cationic derivatives, shown to be due to the electrostatic interaction (He, Davis, & Illum, 1998; Jintapattanakit, Mao, Kissel, & Junyaprasert, 2008). To conclude, the level of adhesion appears to be determined by at least two factors, with the major parameter being the presence of GRGDS-peptides acting as binding sites for the cells. Secondly, the physico-chemical properties of the polymer, such as charge, influence the degree of adhesion in a non-specific manner.

3.4. Cell morphology

In addition to an increased level of cell attachment to GRGDS-CM-TM-chitosan in comparison to SDGRG-CM-TM-chitosan, the morphology of the cells was remarkably different on the different coatings. In the wells with a polymer presenting GRGDS-peptides, the majority of the cells spread and displayed a flat phenotype, whereas the cells on the coatings with the scrambled peptide were of spherical phenotype. These observations indicated an interaction between the GRGDS-moieties and the integrins, causing a re-arrangement of the cytoskeleton and subsequently spreading of the cell. To further investigate the morphology of the HDF during the initial adhesion, the F-actin and the nuclei of the cells were stained with phalloidin conjugated Alexa 488 (green) and DAPI (blue), respectively, after adhesion assays (Fig. 6).

Cells plated on GRGDS-CM-TM-chitosan coatings were compared to cells plated on SDGRG-CM-TM-chitosan. Moreover, cells plated on GRGDS-CM-TM-chitosan under normal conditions and under competitive inhibition conditions were analyzed to confirm the interaction between GRGDS and RGD-dependent integrin receptors. In order to assess the degree of spreading, the mean cell

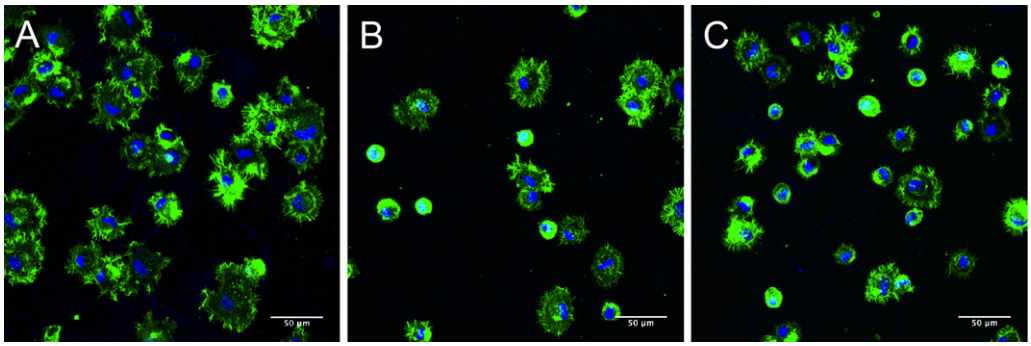

Fig. 6. Confocal images of human dermal fibroblasts (HDF) stained with phalloidin conjugated Alexa 488 (green) and DAPI (blue) for visualization of cytoskeletal actin-filaments and the nuclei, respectively. The images represent the morphology of the cells 30 min after seeding onto GRGDS-CM-TM-chitosan coating under normal conditions (A) or in the presence of free GRGDS (B) and onto a coating of SDGRG-CM-TM-chitosan (C). (For interpretation of the references to color in this figure legend, the reader is referred to the web version of the article.)

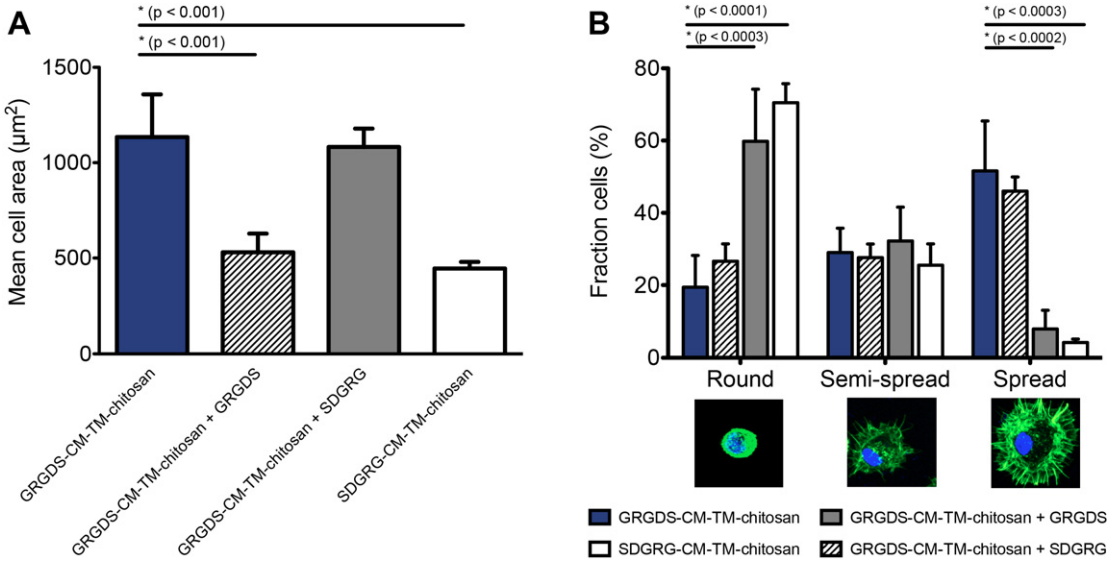

Fig. 7. Cell morphology of HDF after 30 min incubation on coatings of GRGDS-CM-TM-chitosan, SDGRG-CM-TM-chitosan and on GRGDS-CM-TM-chitosan in the presence of 1 mM GRGDS- or SDGRG-peptide (competitive inhibition). (A) Mean cell area in μm^2 ($n = 5$ assays), (B) Classification of cells based on their cell surface area, round cells (<500 μm^2), semi-spread cells (501–1000 μm^2) and fully spread cells (>1000 μm^2). The means ± SD are corresponding to 5 assays.

surface area of the cells was determined for the different conditions, as shown in Fig. 7A. The mean surface ($n = 5$ assays) of the cells plated onto GRGDS-CM-TM-chitosan was $1134 \pm 224\ \mu m^2$, whereas the cells plated onto SDGRG-CM-TM-chitosan had a mean surface of $445 \pm 35\ \mu m^2$. The significant size difference indicated two distinctly different morphologies of the cells as a result of the coating they were placed on. Furthermore, competitive inhibition was used as a method to show specific RGD-dependent cellular interactions. In the presence of free GRGDS in solution (1 mM), the mean cell surface decreased to $530 \pm 98\ \mu m^2$ and hence the spreading was successfully inhibited. On the other hand, the presence of free SDGRG (1 mM) did not inhibit cell spreading, proving the specificity of the GRGDS-peptide.

In Fig. 7B, the distribution of cell morphology is shown. Depending on their surface area, the cells were divided into three groups. Cells with a surface area of less then 500 μm^2 were marked as non-spread, round cells, cells between 500–1000 μm^2 were marked as semi-spread and cells above 1000 μm^2 as fully spread cells. When plated on GRGDS-CM-TM-chitosan coatings, the majority of cells showed semi- or fully spread phenotypes, whereas only 19 ± 9% of the cells were completely round. For the cells seeded on SDGRG-CM-TM-chitosan, 70 ± 5% of the cells were non-spread and only 4 ± 1% of the cells had a surface area exceeding 1000 μm^2. Furthermore, free GRGDS-peptide added to the media was shown to efficiently inhibit spreading of HDF by competitive binding. In the presence of GRGDS, the number of fully spread cells decreased significantly from 52 ± 14% under normal conditions, to only 8 ± 5% ($p < 0.0002$). The number of round cells increased significantly to 60 ± 15% compared to 19 ± 9% under normal conditions ($p < 0.0003$).

The presence of the inactive sequence SDGRG did not have any significant effect on the extent of spreading. Taken together, these results suggest that in addition to increasing the level of adhesion, the GRGDS-moieties grafted onto chitosan polymer induced spreading of the cells during the early adhesion step. This is an important parameter for the cell–biomaterial interaction and also a promising sign for successive interaction.

Chitosan and its derivatives have earlier been shown to have positive effects on the wound healing process and the scar formation. Herein, we show the feasibility of adding an RGD-containing moiety to the chitosan backbone and the positive effects it brings to the early adhesion step and cell–biomaterial interaction.

4. Conclusions

Functionalization of a CM-TM-chitosan with an RGD peptide sequence was shown to direct the behavior of human dermal fibroblasts *in vitro* and increase interaction between the biomaterial and the surrounding tissue. GRGDS-CM-TM-chitosan was well tolerated by the cells and the RGD-moiety increased the level of adhesion of the cells. Additionally, the cells were triggered to spread during the initial adhesion and therefore increased the possibilities of a further successful cell–biomaterial interaction.

Acknowledgements

A. Hansson was a recipient of a 3 years Ph.D. studentship from the Ministère de l'Education (France) and of a Region Rhône-Alpes Explo'ra Doc grant (France). The authors would like to thank Dr. Lee Ann Laurent-Applegate (CHUV, Lausanne, Switzerland) for the kind donation of human dermal fibroblasts. We thank Jean-Pierre Andrieu, from the IBS-platform of the Partnership for Structural Biology and the Institut de Biologie Structurale in Grenoble (PSB/IBS), for the assistance and access to Amino Acids determination facility. We are grateful to Dr. Elisabeth Rivara-Minten (University of Geneva, Switzerland) for helpful discussions and her technical support with the NMR.

References

Alves, N. M., & Mano, J. F. (2008). Chitosan derivatives obtained by chemical modifications for biomedical and environmental applications. *International Journal of Biological Macromolecules*, *43*(5), 401–414.

Amidi, M., Mastrobattista, E., Jiskoot, W., & Hennink, W. E. (2010). Chitosan-based delivery systems for protein therapeutics and antigens. *Advanced Drug Delivery Reviews*, *62*(1), 59–82.

An, N. T., Thien, D. T., Dong, N. T., & Dung, P. L. (2009). Water-soluble N-carboxymethylchitosan derivatives: Preparation, characteristics and its application. *Carbohydrate Polymers*, *75*(3), 489–497.

Bacakova, L., Filova, E., Parizek, M., Ruml, T., & Svorcik, V. (2011). Modulation of cell adhesion, proliferation and differentiation on materials designed for body implants. *Biotechnology Advances*, *29*(6), 739–767.

Baldrick, P. (2010). The safety of chitosan as a pharmaceutical excipient. *Regulatory Toxicology and Pharmacology*, *56*(3), 290–299.

Boucard, N., Viton, C., Agay, D., Mari, E., Roger, T., Chancerelle, Y., et al. (2007). The use of physical hydrogels of chitosan for skin regeneration following third-degree burns. *Biomaterials*, *28*(24), 3478–3488.

Chen, X.-G., & Park, H.-J. (2003). Chemical characteristics of O-carboxymethyl chitosans related to the preparation conditions. *Carbohydrate Polymers*, *53*(4), 355–359.

Danen, E. H., & Sonnenberg, A. (2003). Integrins in regulation of tissue development and function. *The Journal of Pathology*, *201*(4), 632–641.

Denuziere, A., Ferrier, D., Damour, O., & Domard, A. (1998). Chitosan–chondroitin sulfate and chitosan–hyaluronate polyelectrolyte complexes: Biological properties. *Biomaterials*, *19*(14), 1275–1285.

Graf, J., Ogle, R. C., Robey, F. A., Sasaki, M., Martin, G. R., Yamada, Y., et al. (1987). A pentapeptide from the laminin B1 chain mediates cell adhesion and binds the 67,000 laminin receptor. *Biochemistry*, *26*(22), 6896–6900.

He, P., Davis, S. S., & Illum, L. (1998). In vitro evaluation of the mucoadhesive properties of chitosan microspheres. *International Journal of Pharmaceutics*, *166*(1), 75–88.

Hersel, U., Dahmen, C., & Kessler, H. (2003). RGD modified polymers: Biomaterials for stimulated cell adhesion and beyond. *Biomaterials*, *24*(24), 4385–4415.

Heuking, S., Iannitelli, A., Di Stefano, A., & Borchard, G. (2009). Toll-like receptor-2 agonist functionalized biopolymer for mucosal vaccination. *International Journal of Pharmaceutics*, *381*(2), 97–105.

Hjerde, R. J. N., Vårum, K. M., Grasdalen, H., Tokura, S., & Smidsrod, O. (1997). Chemical composition of O-(carboxymethyl)-chitins in relation to lysozyme degradation rates. *Carbohydrate Polymers*, *34*(3), 131–139.

Huveneers, S., & Danen, E. H. (2009). Adhesion signaling—Crosstalk between integrins, Src and Rho. *Journal of Cell Science*, *122*(Pt 8), 1059–1069.

Hynes, R. O. (2009). The extracellular matrix: Not just pretty fibrils. *Science*, *326*(5957), 1216–1219.

Jintapattanakit, A., Mao, S., Kissel, T., & Junyaprasert, V. B. (2008). Physicochemical properties and biocompatibility of N-trimethyl chitosan: Effect of quaternization and dimethylation. *European Journal of Pharmaceutics and Biopharmaceutics: Official Journal of Arbeitsgemeinschaft fur Pharmazeutische Verfahrenstechnik e.V*, *70*(2), 563–571.

Jollès, P., & Muzzarelli, R. A. A. (Eds.). (1999). *Chitin and chitinases*. Basel: Birkhauser Verlag.

Knight, C. G., Morton, L. F., Peachey, A. R., Tuckwell, D. S., Farndale, R. W., & Barnes, M. J. (2000). The collagen-binding A-domains of integrins alpha(1)beta(1) and alpha(2)beta(1) recognize the same specific amino acid sequence, GFOGER, in native (triple-helical) collagens. *The Journal of Biological Chemistry*, *275*(1), 35–40.

Li, W., Fan, J., Chen, M., & Woodley, D. T. (2004). Mechanisms of human skin cell motility. *Histology and Histopathology*, *19*(4), 1311–1324.

Lord, M. S., Cheng, B., McCarthy, S. J., Jung, M., & Whitelock, J. M. (2011). The modulation of platelet adhesion and activation by chitosan through plasma and extracellular matrix proteins. *Biomaterials*, *32*(28), 6655–6662.

Massia, S. P., & Hubbell, J. A. (1991). An RGD spacing of 440 nm is sufficient for integrin alpha V beta 3-mediated fibroblast spreading and 140 nm for focal contact and stress fiber formation. *The Journal of Cell Biology*, *114*(5), 1089–1100.

Murakami, K., Aoki, H., Nakamura, S., Nakamura, S., Takikawa, M., Hanzawa, M., et al. (2010). Hydrogel blends of chitin/chitosan, fucoidan and alginate as healing-impaired wound dressings. *Biomaterials*, *31*(1), 83–90.

Muzzarelli, R. A. A. (1988). Carboxymethylated chitins and chitosans. *Carbohydrate Polymers*, *8*(1), 1–21.

Muzzarelli, R. A. A. (2009). Chitins and chitosans for the repair of wounded skin, nerve, cartilage and bone. *Carbohydrate Polymers*, *76*(2), 167–182.

Muzzarelli, R. A. A. (2011). Chitosan composites with inorganics, morphogenetic proteins and stem cells, for bone regeneration. *Carbohydrate Polymers*, *83*(4), 1433–1445.

Muzzarelli, R. A. A., Greco, F., Busilacchi, A., Sollazzo, V., & Gigante, A. (2012). Chitosan, hyaluronan and chondroitin sulfate in tissue engineering for cartilage regeneration: A review. *Carbohydrate Polymers*, *89*(3), 723–739.

Muzzarelli, R. A. A., & Muzzarelli, C. (2005). Chitosan chemistry: Relevance to the biomedical sciences. In T. Heinze (Ed.), *Advances in polymer science* (pp. 151–209). Berlin: Springer Verlag.

Pierschbacher, M. D., & Ruoslahti, E. (1984). Cell attachment activity of fibronectin can be duplicated by small synthetic fragments of the molecule. *Nature*, *309*(5963), 30–33.

Pretsch, E., Bühlmann, P., & Affolter, C. (2000). *Structure determination of organic compounds: Tables of spectral data*. Berlin: Springer.

Scherer, S. S., Pietramaggiori, G., Matthews, J., Perry, S., Assmann, A., Carothers, A., et al. (2009). Poly-N-acetyl glucosamine nanofibers: A new bioactive material to enhance diabetic wound healing by cell migration and angiogenesis. *Annals of Surgery*, *250*(2), 322–330, 310.1097/SLA.1090b1013e3181ae1099d1045.

Takei, T., Nakahara, H., Ijima, H., & Kawakami, K. (2012). Synthesis of a chitosan derivative soluble at neutral pH and gellable by freeze–thawing, and its application in wound care. *Acta Biomaterialia*, *8*(2), 686–693.